34th EUROPEAN ROTORCRAFT FORUM

Session: Flight Mechanics

IN-FLIGHT ESTIMATION OF HELICOPTER GROSS WEIGHT AND MASS CENTER LOCATION

by

M. Abraham, M. Costello

School of Aerospace Engineering
Georgia Institute of Technology
Atlanta, Georgia 30332

SEPTEMBER 16-19, 2008
LIVERPOOL
ENGLAND

IN-FLIGHT ESTIMATION OF HELICOPTER GROSS WEIGHT AND MASS CENTER LOCATION

Michael Abraham,* Mark Costello$

School of Aerospace Engineering

Georgia Institute of Technology

Atlanta, Georgia 30327

Abstract

The ability to compute the weight and balance of a helicopter in flight under general conditions is an enabling technology for future condition based maintenance systems as well as advanced automatic flight control systems. This paper creates a real-time weight and balance estimation algorithm using an extended Kalman filter framework. To highlight estimation characteristics, the algorithm is exercised on the OH-6A helicopter in a variety of flight regimes. The algorithm is shown to work well in hover and forward flight as well as situations where loads are dropped and picked up in flight. Typically the algorithm quickly estimates station line and butt line mass center position (1 sec) and more slowly converges on helicopter weight (10 sec). To estimate helicopter waterline, the algorithm requires maneuvering flight where non zero roll rate is present. The algorithm is also shown to be reasonably robust to sensor and model errors.

NOMENCLATURE

x, y, z : Components of helicopter mass center position vector in an inertial frame.

ϕ, θ, ψ : Euler roll, pitch and yaw angles of helicopter.

u, v, w : Components of mass center velocity of helicopter in the helicopter reference frame.

p, q, r : Components of angular velocity of helicopter in the helicopter reference frame.

m, W : Mass and weight of helicopter.

I_H : Inertia matrix of helicopter about its mass center.

I_B : Flapping inertia of rotor blade.

X, Y, Z : Total force on the helicopter in the helicopter reference frame.

L, M, N : Total moment on the helicopter about the mass center in the helicopter reference frame.

T_H : Transformation matrix from inertial reference frame to helicopter reference frame.

$\beta, \beta_0, \beta_{1C}, \beta_{1S}$: Flapping angle, collective, longitudinal, lateral flapping angles.

R : Rotor radius.

INTRODUCTION

It is well known that weight and mass center location greatly affect static and dynamic characteristics of helicopters. These quantities are often manipulated during the design process to obtain desired performance from the aircraft. Safe operation of helicopters is a function of not only the weight of the aircraft but also the location of the mass center. Sufficiently accurate in-flight estimation of the gross weight and mass center location can substantially improve overall performance of the air vehicle as these feedback signals can be put to good use within a condition based maintenance system, a health and usage monitoring system, and the automatic flight control system. Determining the useful life of parts on helicopters relies on knowledge of how long the aircraft is in a given flight condition so that damage on components can be properly tallied. Since

* Graduate Research Assistant.

$ Sikorsky Associate Professor.

damage on components is a strong function of gross weight and mass center location, accurate and relatively frequent in-flight estimation of gross weight and mass center location help markedly enhance safety and reduce the operating cost of helicopters by removing parts on the aircraft at the end of their useful life and avoid replacing parts too early or leaving them on the aircraft too long. Real-time weight and balance information can also be used for flight control. This is particularly true for heavy lift helicopters where it may be necessary to schedule gains in the flight control system as a function of the gross weight and mass center location to ensure adequate handling qualities over the operational envelope of the aircraft and to also insure integrity of the airframe by altering control inputs to limit flight loads on the structure.

A simple way to estimate the weight and mass center of a helicopter is to use weight on wheels information before take-off combined with fuel burn measurements. While simple and straightforward, this method cannot be used in cases where loads are dropped off or picked up in flight – a common operation for rotorcraft, particularly heavy lift rotorcraft. More sophisticated methods have been developed, but all suffer from considerable limitations that preclude general use. Moffatt [1] created a simple algorithm to predict the weight of a helicopter which requires only engine torque, hover height, pressure altitude and ambient temperature. The algorithm is based on the UH-1H hover performance chart found in the operator user manual. Morales and Haas [2] created a neural network algorithm to estimate the weight of a helicopter in hover. Although this work only addressed the hover flight regime, it showed the ability of neural networks to be properly trained on noisy flight test data and subsequently employed for in-flight gross weight estimation. Idan, Iosilevskii, and Nazarov [3] also created a neural network based method to estimate gross weight along with the mass center of an aircraft in-flight. To speed the training process for the neural network, basic flight mechanics relations were incorporated into the algorithm. While Moffatt [1] as well as Morales and Haas [2] focused weight estimation for helicopters, neither algorithm is valid in forward flight and neither addresses mass center location prediction. Inversely, the work of Idan, Iosilevskii, and Nazarov [3] estimates both weight and mass center location, however, it is strickly applicable to commercial fixed wing aircraft.

The work reported here presents a new algorithm for real-time in-flight estimation of helicopter gross weight and mass center location. An extended Kalman filter is constructed with the rigid state of the aircraft as states along with the weight and three components of the mass center. A unique feature of the algorithm relative to existing methods is its generally applicability, including scenarios where the weight and balance changes due to dropping off and picking up loads. The developed algorithm is exercised on the OH6A helicopter and results are presented as a function of different maneuvers and different levels of model and sensor error.

HELICOPTER DYNAMIC MODEL

For the work reported below, helicopter motion is simulated by modeling the aircraft as a rigid body with six degrees of freedom. The state vector consists of twelve state variables that describe position and velocity of the vehicle's mass center and the attitude and angular rates of the vehicle with respect to inertial space.

$$\begin{Bmatrix} \dot{x} \\ \dot{y} \\ \dot{z} \end{Bmatrix} = \left[T_H \right] \begin{Bmatrix} u \\ v \\ w \end{Bmatrix} \tag{1}$$

$$\begin{Bmatrix} \dot{\phi} \\ \dot{\theta} \\ \dot{\psi} \end{Bmatrix} = \begin{bmatrix} 1 & s_\phi t_\theta & c_\phi t_\theta \\ 0 & c_\phi & -s_\phi \\ 0 & s_\phi / c_\theta & c_\phi / c_\theta \end{bmatrix} \begin{Bmatrix} p \\ q \\ r \end{Bmatrix} \tag{2}$$

$$\begin{Bmatrix} \dot{u} \\ \dot{v} \\ \dot{w} \end{Bmatrix} = \begin{Bmatrix} X/m \\ Y/m \\ Z/m \end{Bmatrix} + \begin{bmatrix} 0 & -r & q \\ r & 0 & -p \\ -q & p & 0 \end{bmatrix} \begin{Bmatrix} u \\ v \\ w \end{Bmatrix} \quad (3)$$

$$\begin{Bmatrix} \dot{p} \\ \dot{q} \\ \dot{r} \end{Bmatrix} = [I_H]^{-1} \left[\begin{Bmatrix} L \\ M \\ N \end{Bmatrix} - [S_H][I_H] \begin{Bmatrix} p \\ q \\ r \end{Bmatrix} \right] \quad (4)$$

where

$$T_H = \begin{bmatrix} c_\theta c_\psi & c_\theta s_\psi & -s_\theta \\ s_\phi s_\theta c_\psi - c_\phi s_\psi & s_\phi s_\theta s_\psi + c_\phi c_\psi & s_\phi c_\theta \\ c_\phi s_\theta c_\psi + s_\phi s_\psi & c_\phi s_\theta c_\psi - s_\phi c_\psi & c_\phi c_\theta \end{bmatrix}$$

$$S_H = \begin{bmatrix} 0 & -r & q \\ r & 0 & -p \\ -q & p & 0 \end{bmatrix}$$

In the above equations the normal shorthand notation for sine and cosine is employed: $s_\alpha = \sin(\alpha)$, $c_\alpha = \cos(\alpha)$.

The total forces and moments in the helicopter reference frame that appear in Equations 3 and 4 have contributions from helicopter weight, the main rotor, the tail rotor, fuselage aerodynamics, and empenage aerodynamics. Forces from each component are first found in that component's reference frame and then are transformed into the vehicle's body frame. Moment contributions from each component come from two sources: pure moments and moments due to the offset of the component's forces from the vehicle's center of mass.

The rotor model that is used for both the main rotor and tail rotor uses a quasi-state combined blade-element/momentum-theory approach. The model assumes rigid blades but accounts for twist, taper and nonzero flapping hinge offset. First harmonic flapping and uniform inflow is assumed.

$$\beta = \beta_0 + \beta_{1C}\cos(\psi_{MR}) + \beta_{1S}\sin(\psi_{MR}) \quad (5)$$

The differential equation that governs rotor flapping dynamics is given below.

$$\ddot{\beta} + \omega_N^2 \beta = M_F \quad (6)$$

where

$$\omega_N = \Omega \sqrt{\frac{I_B + \frac{m e R}{2}}{I_B}} \quad (7)$$

$$M_F = -\frac{M_A}{I} - \frac{mgR}{2I} \quad (8)$$

At a given instant in time the quasi-steady rotor flapping angles, and subsequently the rotor loads, are computed by a harmonic balance procedure. Nonlinear algebraic collective, longitudinal, and lateral rotor flapping equations are formed as shown below.

$$\int_0^{2\pi} \left(\ddot{\beta} + \omega_N^2 \beta - M_F \right) d\psi_{MR} = 0 \quad (9)$$

$$\int_0^{2\pi} \left(\ddot{\beta} + \omega_N^2 \beta - M_F \right) c_{\psi_{MR}} \, d\psi_{MR} = 0 \quad (10)$$

$$\int_0^{2\pi} \left(\ddot{\beta} + \omega_N^2 \beta - M_F \right) s_{\psi_{MR}} \, d\psi_{MR} = 0 \quad (11)$$

These equations are satisfied through selection of the rotor flapping angles β_0, β_{1C} and β_{1S} and are numerically solved by a Newton-Rhapson iteration scheme. It is important to note that pilot controls enter the rotor flapping equations through the right hand side forcing function.

Force and moment contributions from the fuselage and empenage are modeled with aerodynamic table lookups.

ESTIMATION ALGORITHM

The estimation algorithm seeks to compute the mass of the helicopter along with the three components of the mass center locations using rigid body aircraft motion feedback and an internal model of the helicopter (Figure 1).

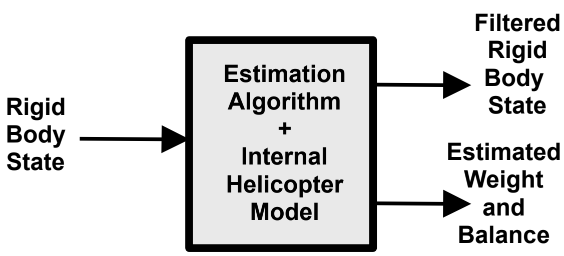

Figure 1 – Estimation Algorithm Schematic

An extended Kalman filter is created with rigid aircraft position (x, y, z), orientation (phi, theta, psi), translational velocity (u, v, w), angular velocity (p, q, r), aircraft mass (m), and aircraft mass center location (scg, bcg, wcg) as states. The nonlinear helicopter model described above is used for the internal aircraft model. The weight and balance of the helicopter is assumed to vary relatively slowly so the dynamics of the weight and balance states are trivially assumed to be given below.

$$\dot{m} = 0 \tag{12}$$

$$\dot{x}_{CG} = 0 \tag{13}$$

$$\dot{y}_{CG} = 0 \tag{14}$$

$$\dot{z}_{CG} = 0 \tag{15}$$

The meta model of helicopter rigid body motion and weight and balance estimation states is cast together as a nonlinear dynamic system.

$$\dot{\zeta} = f(\zeta, \delta) + \varepsilon(t) \tag{16}$$

The vector δ contains control inputs consisting of collective, longitudinal cyclic, lateral cyclic and pedal. The vector ε is process noise. The meta state is split into the helicopter rigid body state and the mass and balance state, $\zeta = [\zeta_H \quad \zeta_E]^T$.

$$\zeta_H = \begin{Bmatrix} x \\ y \\ z \\ \phi \\ \theta \\ \psi \\ u \\ v \\ w \\ p \\ q \\ r \end{Bmatrix} \qquad \zeta_E = \begin{Bmatrix} m \\ x_{CG} \\ y_{CG} \\ z_{CG} \end{Bmatrix} \tag{17}$$

Measurements of rigid body motion of the helicopter used as input to the estimation algorithm contain rigid body motion and noise.

$$\eta = h(\zeta, \delta) + \kappa(t) \tag{18}$$

In the equation above, $\kappa(t)$ represents a vector of measurement noise.

Given the nonlinear system model above, an extended Kalman filter has 5 main steps associated with each estimation cycle: meta state propagation, meta state error covariance propagation, Kalman gain calculation, meta state Kalman filter update, meta state error covariance Kalman filter update. This is depicted in Figure 2.

Several of the steps in the Kalman filter require a linear state space dynamic model and a linear measurement model.

$$\dot{\zeta}(t) = A\zeta(t) + B\delta(t) \qquad (19)$$

$$\eta(t) = C\zeta(t) \qquad (20)$$

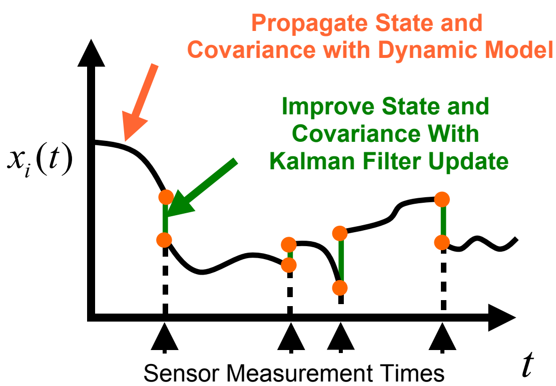

Figure 2 – Kalman Filter Schematic

Of course, the state dynamic equations are highly nonlinear and a numerical, finite difference approach is used to obtain the needed derivatives for the linear time invarient dynamic model.

$$A = \frac{\partial f}{\partial \zeta}, B = \frac{\partial f}{\partial \delta}, C = \frac{\partial h}{\partial \zeta} \qquad (21)$$

The meta state of the system is propogated forward in time by numerically integrating the equations of motion (Equation 16) with the process noise set to zero. The error covariance differential equation (Equation 22) is also numerically integrated in time to propagate itself forward.

$$\dot{P} = AP + PA^T + Q - PH^T R^{-1} HP \qquad (22)$$

Because the initial state is assumed known, the matrix P is initially zero. In the above equation, Q and R are the covariance matrices for the process noise and measurement noise, respectively. The performance of this filtering technique depends largely upon the selected values for Q and R. Because the parameter estimation process is cast in the guise of a state estimation process, the Q matrix must be weighted heavily toward the unknown parameter states.

The Kalman gain formula is given as Equation 23. Aside from the linearization process of the helicopter plant, this step is the most expensive in terms of computing power. If full state feedback is assumed, a 12x12 matrix must be inverted at each computation cycle.

$$K = PH^T \left[HPH^T + R \right]^{-1} \qquad (23)$$

Using the Kalman gain matrix, state and error covariance can be computed as shown below.

$$\tilde{\zeta} = \zeta + K[\eta - C\zeta] \qquad (24)$$

$$\tilde{P} = [I - KH] P [I - KH]^T + KRK^T \qquad (25)$$

The tilde in Equations 24 and 25 refers to values of the state and error covariance after the Kalman update step.

More details on the extended Kalman filter can be found in References [4] and [5].

RESULTS

To explore the viability of the above estimation scheme for real time, in-flight helicopter gross weight and mass center location prediction, a set of simulation results have been generated for the OH-6A helicopter shown in Figure 3. The OH-6A is a single-engine light helicopter with a four-bladed main rotor used for personnel transport, escort and attack missions, and observation. The main rotor has a non-dimensional twist of -0.14, a flapping hinge offset of 0.46 ft, a radius of 13.17 ft, a rotational speed of 50.58 rad/sec, a blade mass of 1.16 slugs, a flapping inertia of 46.83 slugs*ft^2, and an average chord of 0.56 ft. The main rotor is located at station line 100.0 in, butt line 0.0 in, and waterline of 100.0 in.

Figure 3 - OH-6A Helicopter

The tail rotor is a two bladed system with a non-dimensional twist of -0.14 and a radius of 1.13 ft, and a rotational speed of 326.1 rad/sec. The tail rotor is located at station line 282.00 in, butt line -11.6 in, and water line 71.3 in. The nominal gross weight of the vehicle is 2550 lbf. The nominal mass center location is station line 100.0 in, butt line 0.0 in, and water line 49.6 in. Fuselage aerodynamic data are shown in Figures 4 and 5 while empenage aerodynamic coefficients are given in Figure 6.

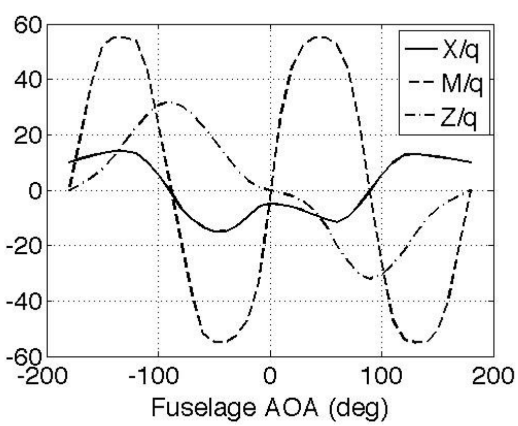

Figure 4 – Fuselage Longitudinal Aerodynamic Data

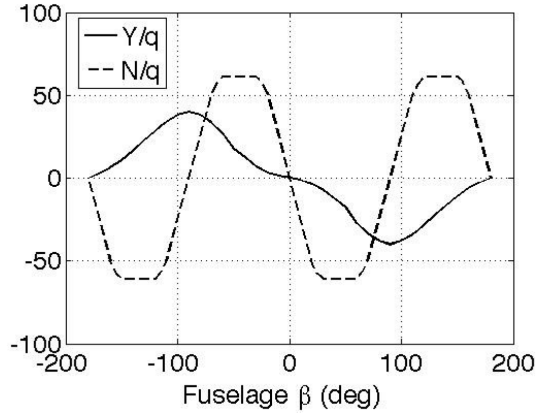

Figure 5 – Fuselage Lateral Aerodynamic Data

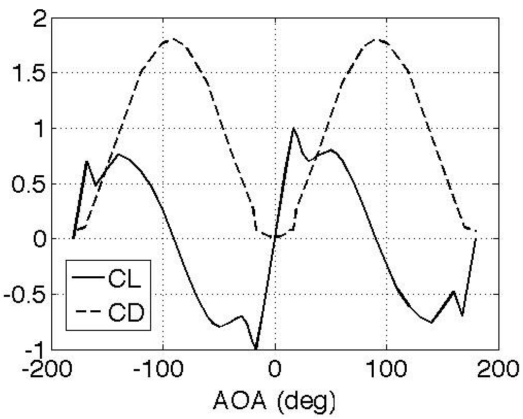

Figure 6 – Empenage Aerodynamic Coefficients

Figures 7 through 23 show the OH-6A in forward flight at a reasonably steady speed (Figures 13-15) and at nearly constant pitch attitude (Figure 11). The aircraft is maneuvering in the lateral channel with roll angle excursions on the order of 50 deg over a 20 sec period, ranging from +20 deg to -30 deg (Figure 10) with associated peak roll rates of 30 deg/sec (Figure 16). The aircraft also has heading oscillations from +20 deg to -40 deg (Figure 12) with peak yaw rates of 7 deg/sec (Figure 18). During this maneuver condition, the aircraft maintains constant altitude (Figure 9) and swerves modestly (Figure 8). Control activity is modest with main rotor collective settling around 12.5 deg and cyclic pitch oscillations of under 2 deg in both channels (Figures 19-21). For the maneuver shown above, weight and balance estimation results are shown in Figures 22 through 25. The estimator is turned on at t = 0 sec with initial gross weight in error by 250 lbf and initial mass center station line, butt line, and water line in error by 2, 2, and 1 in, respectively. The Kalman filter weighting matrices are set to 0.02 for the rotorcraft model, 1000 for the weight and balance model with the exception of water line which is set to 2000, and 1.0 for the measurement noise. Weight and mass center water line are effectively estimated in slightly less than 10 sec (Figures 22 and 25). Converged estimates for mass center station line and butt line occur much more rapidly (Figures 23 and 24). Estimation of mass center water line is tricky and seems to require aircraft roll rate to render the water line observable with the filter. Figure 26 illustrates this point. In Figure 26, a larger initial error of 2 inches in mass center water line and a lower Q matrix weighting of 1000 is shown. By viewing aircraft roll rate (Figure 16) alongside Figure 26 it is clear that estimation of water line requires roll rate to progress toward the actual value. The results shown above are typical for forward flight.

Figures 27 through 30 present estimation results for a hover case in which the weight and mass center location are suddenly changed due to a 500 lbf load added below and to the right of the original mass center location. For the first 2.5 sec of the hover, the vehicle is at baseline values of weight = 2550 lbf, mass center station line = 100 in, mass center butt line = 0.0 in, and mass center water line = 49.6 in. After the weight is added, weight = 3050 lbf, mass center station line = 102 in, mass center butt line = 2.0 in, and mass center water line = 46.4 in. At t = 5 sec, the vehicle begins a benign maneuver in which it picks up a small amount of flight speed and banks a small amount. The Kalman filter weighting matrices are set the same as the forward flight case above, except the Q matrix associated with the weight and balance model equals 2000. During the pure hover portion of the maneuver, the more observable parameters (gross weight, station line, and butt line) perform reasonably well in adjusting to a new weight and balance condition. The less observable parameter (water line) does a poor job. After slight maneuvering occurs at t = 5 sec, the parameter estimates immediately begin correcting themselves as soon as some rates are present. Just like the forward flight case, the water line estimate moves fastest when a roll rate is present.

In order to explore performance of the weight and balance estimation algorithm under non ideal conditions, the algorithm was exercised with a Monte Carlo simulation with sensor and model error. A total of 200 sample runs were performed for a forward flight case with light maneuvering. Sensor errors were included in the Monte Carlo simulation by adding appropriate levels of bias and noise to each sensor output. The standard deviation of the bias and noise of the position, velocity, orientation, and angular velocity sensors was 1 m/1 m, 0.3 m/s/0.3 m/s, 0.1 deg/0.1 deg, and 0.1 rad/sec/0.1 rad/sec, respectively. Figures 31 through 34 show histograms of the Monte Carlo results for the sensor error case. The mean estimation error and associated standard deviation for gross weight (2558.9 lbf / 6.23 lbf), mass center station line (100.005 in / 0.0261 in), and mass center butt line (0.0025 in / 0.0285 in) are accurate and tightly bounded while the water line estimation is fairly poor and exhibits a standard deviation which is a notable percentage of the practical range of the water line (49.55 in / 0.482 in). Model error was included in the Monte Carlo simulation by creating a model mismatch between the actual helicopter model and the internal helicopter model employed by the estimator. Figures 35 through 38 present histograms of Monte Carlo simulation results for the model error case. While the results for all the parameters shows the same trends as the sensor error case, estimation errors are generally larger and also tend to be more skewed.

CONCLUSIONS

By casting estimation of weight and mass center location as a state estimation problem, the machinery of extended Kalman filtering can be employed for in-flight and real time estimation of rotorcraft weight and balance. The presented algorithm is shown to work well in both hover and forward flight, provided sufficient motion is present to render the parameters observable. Also, the method works well in cases where loads are dropped or picked up in flight. Typically the algorithm quickly estimates station line and butt line mass center position and more slowly converges on helicopter weight and water line. The algorithm is also shown to be reasonably robust to sensor and model errors.

REFERENCES

[1] J. Moffatt, "Helicopter Gross Weight Determination from Monitored Parameters," Aviation and Troop Command, Fort Eustis, VA, ADA311339, 1986.

[2] M. Morales, D. Haas, "Feasibility of Aircraft Gross Weight Estimation Using Artificial Neural Networks," Proceedings of the 57th American Helicopter Society International Annual Forum, Alexandria, VA, pp 1872-1880, 2001.

[3] M. Idan, G. Iosilevskii, S. Nazarov, "In-Flight Weight and Balance Identification Using Neural Networks," *Journal of Aircraft*, Vol 41, No 1, pp 137-143, 2003.

[4] R. Stengel, Optimal Control and Estimation, Dover Publications Inc., New York, ISBN 0-486-68200-5, 1986.

[5] P. Kanjilal, Adaptive Prediction and Predictive Control, IEE Control Engineering Series, Peter Peregrinus Ltd, ISBN 0 86341 193 2, 1995.

[6] E. Siegel, "Stability and Control Data Summary for Single Rotor Helicopter, Hughes OH-6A," Hughes Helicopter Report 369-V-8010, April 28, 1975.

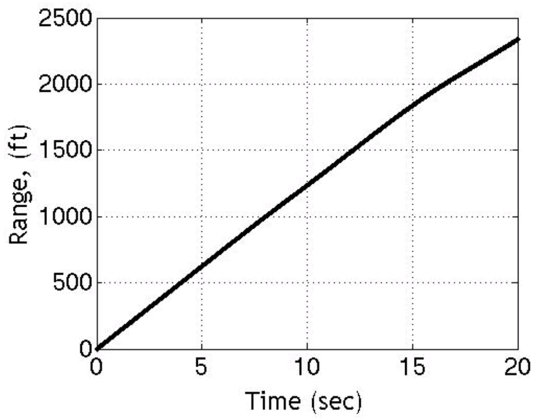

Figure 7 – Down Range Distance

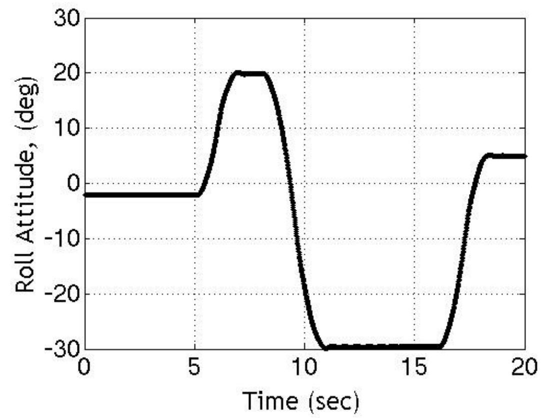

Figure 10 – Roll Angle

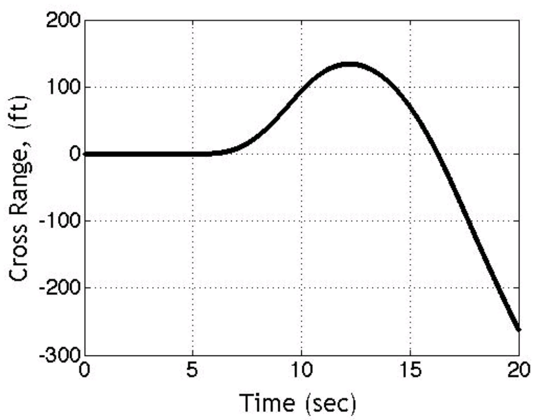

Figure 8 – Cross Range Distance

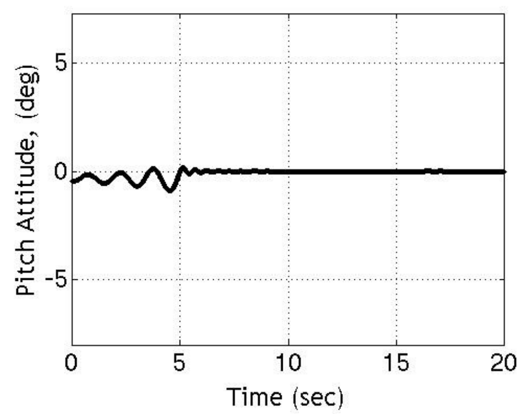

Figure 11 – Pitch Attitude

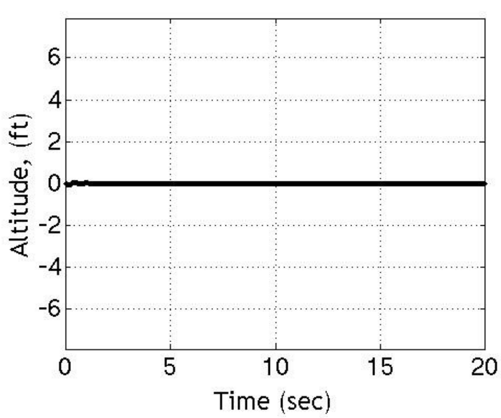

Figure 9 – Altitude

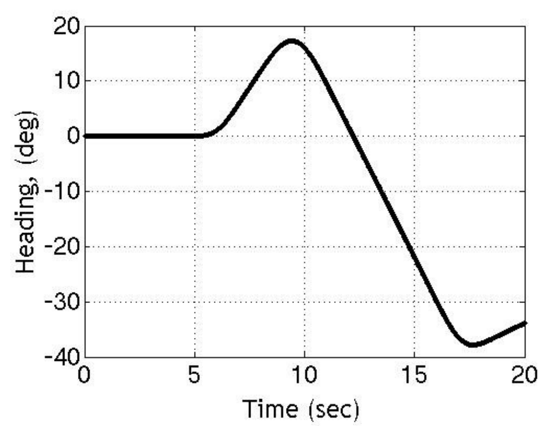

Figure 12 – Yaw Angle

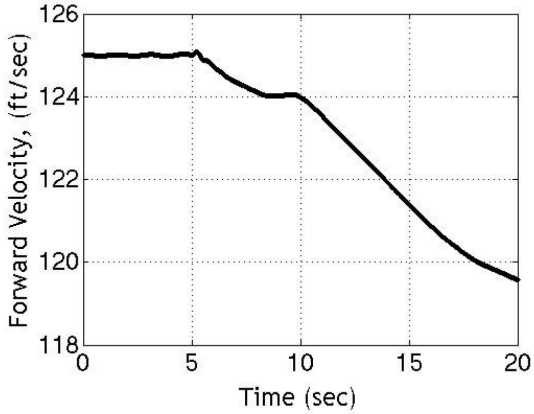

Figure 13 – Forward Body Velocity

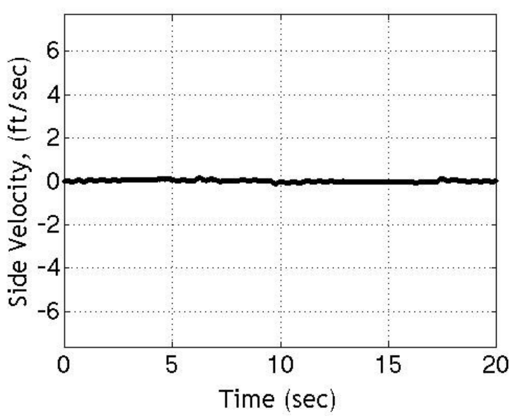

Figure 14 – Side Body Velocity

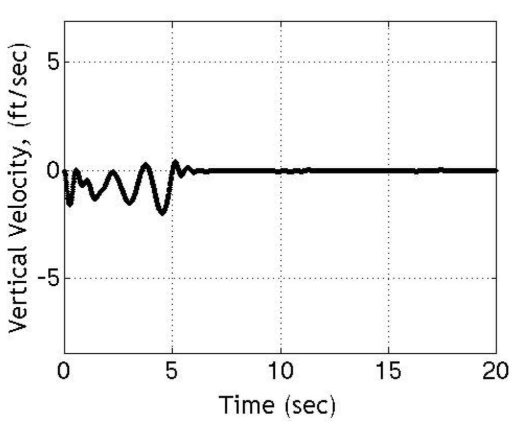

Figure 15 – Vertical Body Velocity

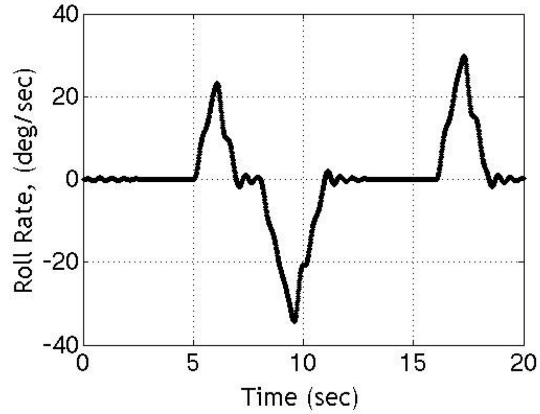

Figure 16 – Roll Rate

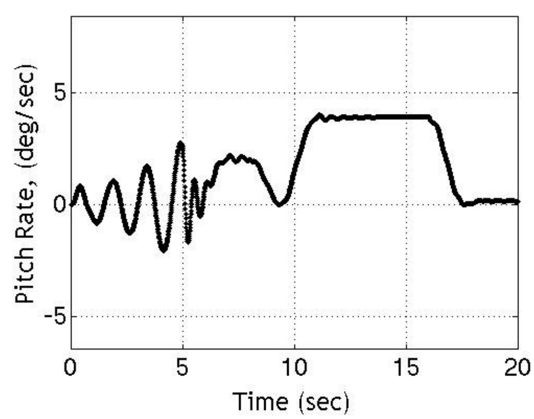

Figure 17 – Pitch Rate

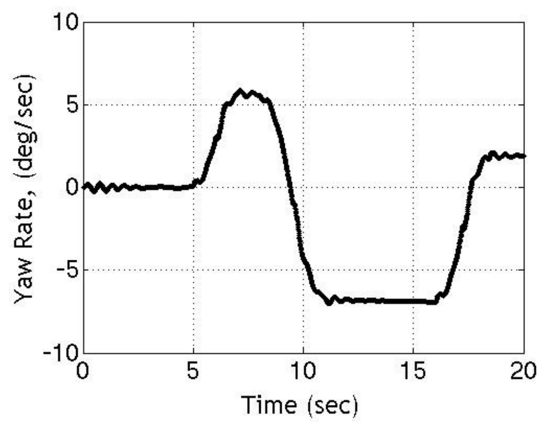

Figure 18 – Yaw Rate

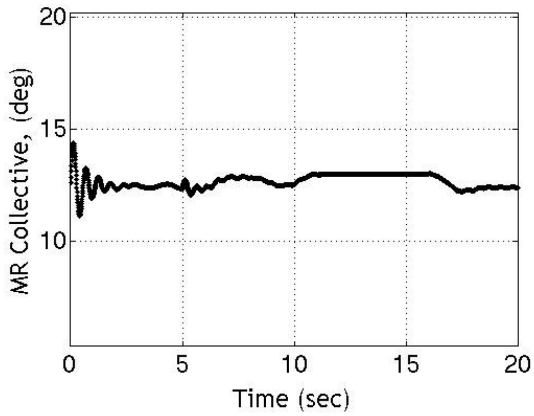

Figure 19 – Main Rotor Collective

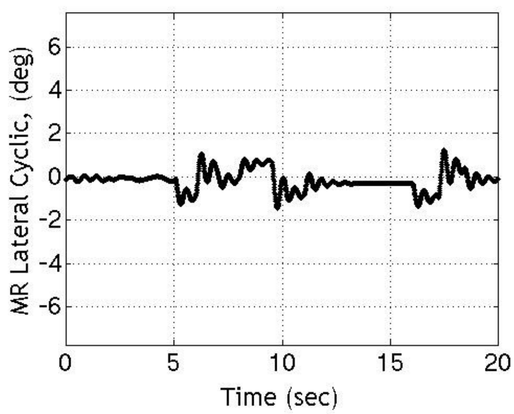

Figure 20 – Main Rotor Longitudinal Cyclic

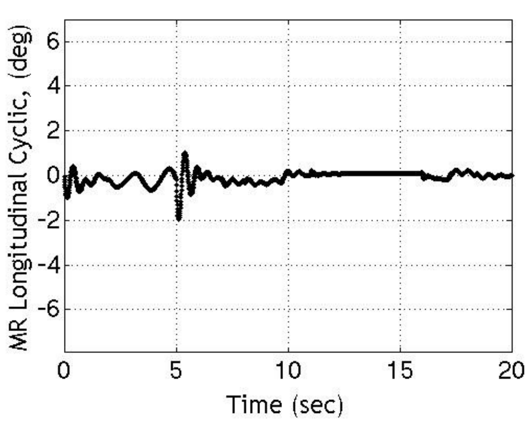

Figure 21 – Main Rotor Lateral Cyclic

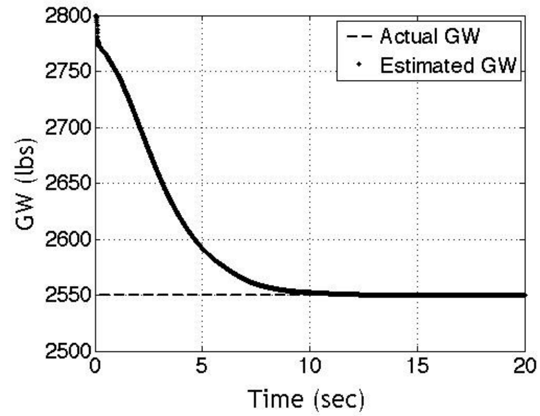

Figure 22 – Gross Weight Estimation in Forward Flight

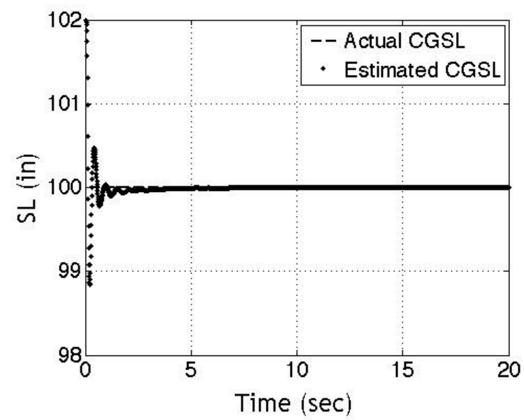

Figure 23 – Mass Center Station line Estimation in Forward Flight

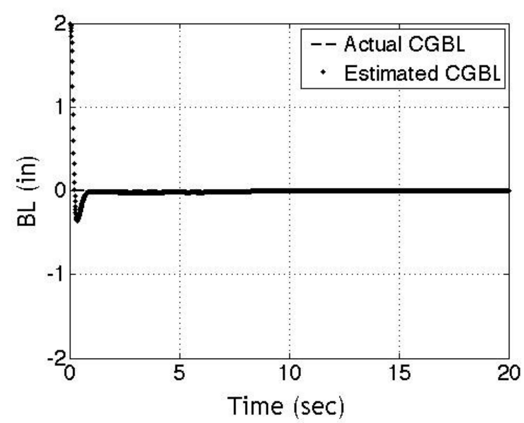

Figure 24 – Mass Center Butt line Estimation in Forward Flight

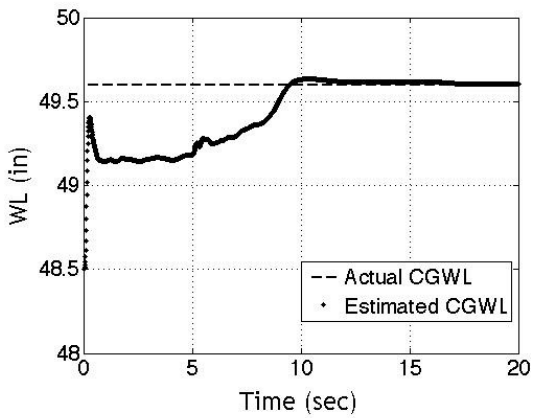

Figure 25 – Mass Center Water line Estimation in Forward Flight

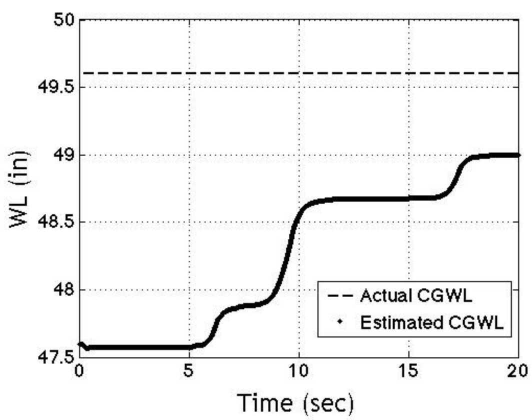

Figure 26 – Mass Center Water line Estimation in Forward Flight (Poor Initial Guess)

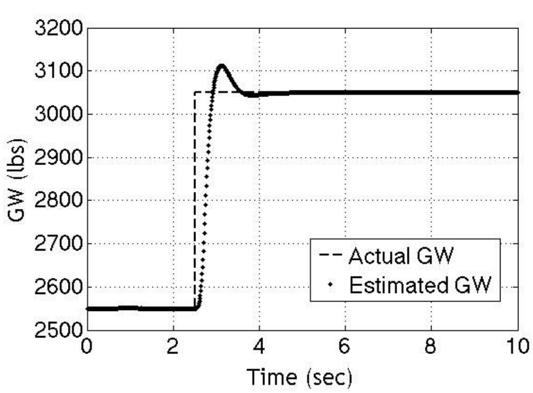

Figure 27 – Gross Weight Estimation in Hover

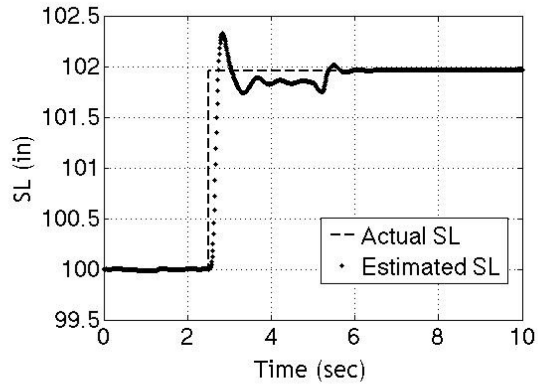

Figure 28 – Mass Center Station line Estimation in Hover

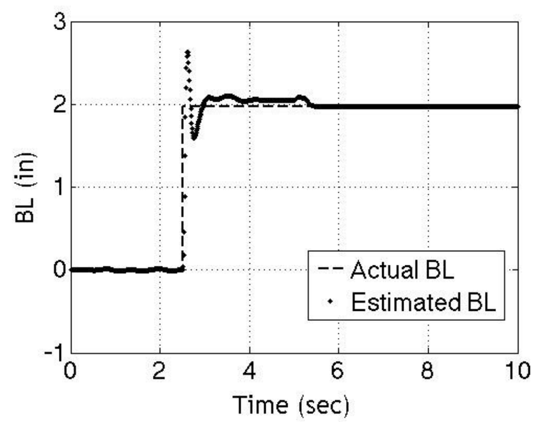

Figure 29 – Mass Center Butt line Estimation in Hover

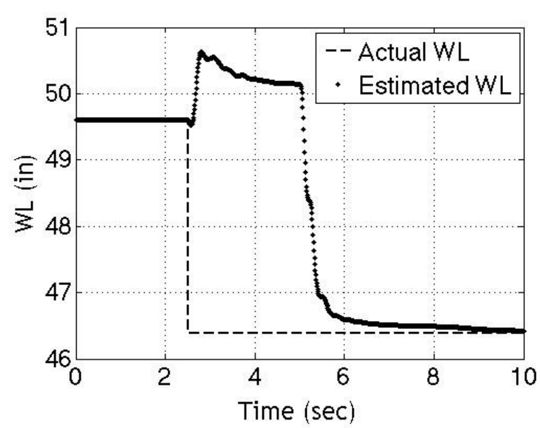

Figure 30 – Mass Center Water line Estimation in Hover

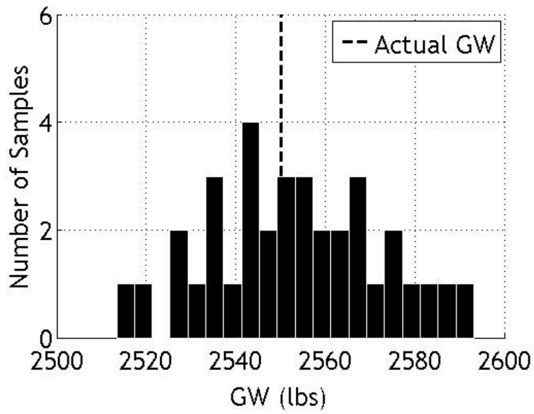

Figure 31 – Histogram of Gross Weight Estimation with Sensor Noise

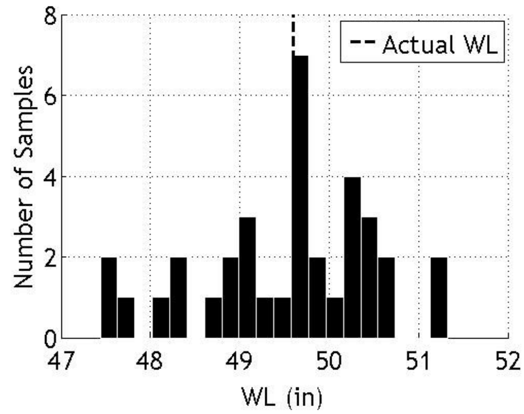

Figure 34 - Histogram of Mass Center Water line Estimation with Sensor Noise

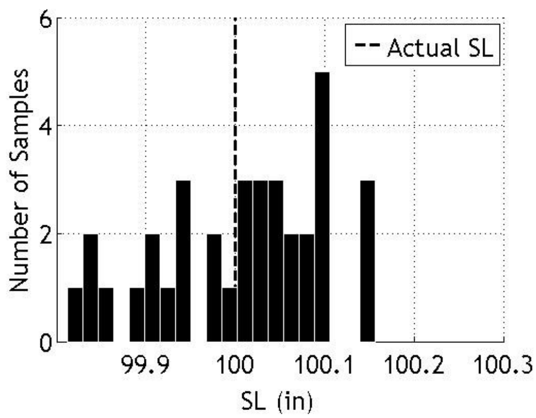

Figure 32 – Histogram of Mass Center Station line Estimation with Sensor Noise

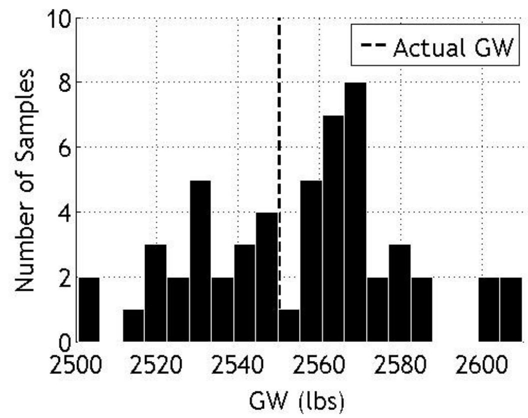

Figure 35 - Histogram of Gross Weight Estimation with Model Error

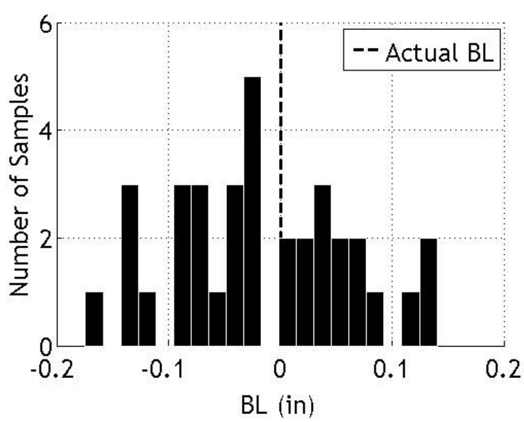

Figure 33 - Histogram of Mass Center Butt line Estimation with Sensor Noise

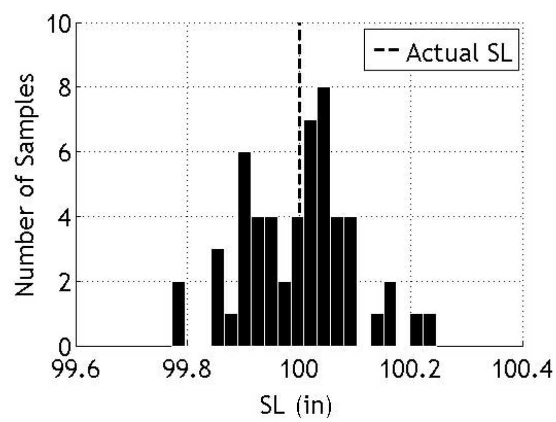

Figure 36 - Histogram of Mass Center Station line Estimation with Model Error

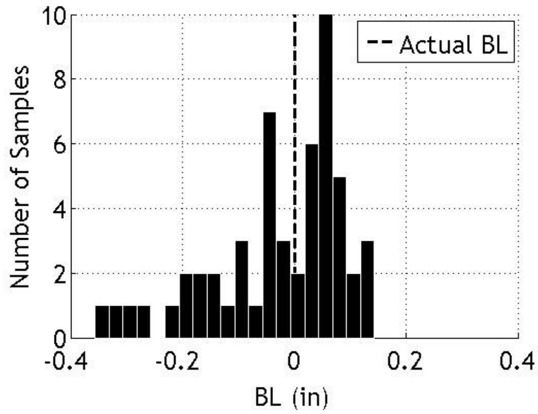

Figure 37 - Histogram of Mass Center Butt line Estimation with Model Error

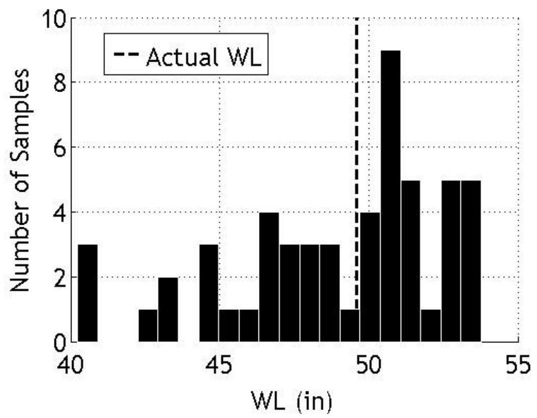

Figure 38 - Histogram of Mass Center Water line Estimation with Model Error